Author Manuscript Published OnlineFirst on April 18, 2019; DOI: 10.1158/0008-5472.CAN-18-3438
Author manuscripts have been peer reviewed and accepted for publication but have not yet been edited.

MDM4 is targeted by 1q gain and drives disease in Burkitt lymphoma

Short title: MDM4 amplification in Burkitt lymphoma

Jennifer Hüllein[1,2], Mikołaj Słabicki[1]*, Maciej Rosolowski[3#], Alexander Jethwa[1,2], Stefan Habringer[4], Katarzyna Tomska[1], Roma Kurilov[5], Junyan Lu[6], Sebastian Scheinost[1], Rabea Wagener[7,8], Zhiqin Huang[9], Marina Lukas[1], Olena Yavorska[6], Hanne Helfrich[10], René Scholtysik[11#], Kyle Bonneau[12], Donato Tedesco[12], Ralf Küppers[11#], Wolfram Klapper[13#], Christiane Pott[14#], Stephan Stilgenbauer[10#], Birgit Burkhardt[15#], Markus Löffler[3#], Lorenz H. Trümper[16#], Michael Hummel[17#], Benedikt Brors[5], Marc Zapatka[9], Reiner Siebert[7,8#], Markus Kreuz[3#], Ulrich Keller[4,18], Wolfgang Huber[6], and Thorsten Zenz[1,19]**[#]; [#]for the MMML consortium

[1]Molecular Therapy in Hematology and Oncology & Department of Translational Oncology, NCT and DKFZ, Heidelberg, Germany
[2]Faculty of Biosciences, Heidelberg University, Heidelberg, Germany
[3]Department for Statistics and Epidemiology, Institute for Medical Informatics, Leipzig, Germany
[4]III. Medical Department of Hematology and Medical Oncology, Technical University of Munich, Germany
[5]Division of Applied Bioinformatics, DKFZ, Heidelberg, Germany
[6]European Molecular Biology Laboratory (EMBL), Heidelberg, Germany
[7]Institute of Human Genetics, Ulm University & Ulm University Medical Center, Germany
[8]Institute of Human Genetics, University of Kiel, Kiel, Germany
[9]Division of Molecular Genetics, DKFZ, Heidelberg, Germany
[10]Department of Internal Medicine III, University of Ulm, Germany
[11]Institute of Cell Biology (Cancer Research), University of Duisburg-Essen, Medical School, Essen, Germany, and the German Cancer Consortium (DKTK)
[12]Cellecta, Inc., Mountain View, CA 94043
[13]Department of Pathology, Hematopathology Section and Lymph Node Registry, University Hospital Schleswig-Holstein, Campus Kiel, Christian-Albrechts-University Kiel, Kiel, Germany
[14]Second Medical Department, University Hospital Schleswig-Holstein, Campus Kiel, Kiel, Germany
[15]Department of Pediatric Hematology and Oncology, NHL-BFM Study Center, University Children's Hospital, Münster, Germany
[16]Department of Hematology and Medical Oncology, Göttingen University Medical Center, Göttingen, Germany
[17]Institute of Pathology, Charité–University Medicine Berlin, Berlin, Germany
[18]Division of Hematology and Oncology at Campus Benjamin Franklin (CBF), Charité, Berlin, Germany
[19]Department of Medical Oncology and Hematology, University Hospital Zurich, Zurich, Switzerland

* Co-first author; ** Lead author

Contact Information

Thorsten Zenz, MD

University Hospital Zürich

Raemistrasse 100

CH-8091 Zürich

Tel +41-44-255 9469

Fax +41-44-255 4560

www.haematologie-onkologie.usz.ch

Email: thorsten.zenz@usz.ch

This manuscript is available on BioRxiv: https://doi.org/10.1101/289363

Conflict of Interest Disclosures

Kyle Bonneau and Donato Tedesco are working for Cellecta Inc., Mountain View, CA, US and provided unpublished RNAi screening data.

Author Manuscript Published OnlineFirst on April 18, 2019; DOI: 10.1158/0008-5472.CAN-18-3438
Author manuscripts have been peer reviewed and accepted for publication but have not yet been edited.

Abstract

Oncogenic MYC activation promotes proliferation in Burkitt lymphoma (BL), but also induces cell cycle arrest and apoptosis mediated by p53, a tumor suppressor that is mutated in 40% of BL cases. To identify molecular dependencies in BL, we performed RNAi-based, loss-of-function screening in eight BL cell lines and integrated non-BL RNAi screens and genetic data. We identified 76 genes essential to BL, including genes associated with hematopoietic cell differentiation (*FLI1*, *BCL11A*) or B cell development and activation (*PAX5*, *CDKN1B*, *JAK2*, *CARD11*) and found a number of context-specific dependencies including oncogene addiction in cell lines with *TCF3*/*ID3* or *MYD88* mutation. The strongest genotype-phenotype association was seen for *TP53*. MDM4, a negative regulator of *TP53*, was essential in *TP53* wild-type (TP53wt) BL cell lines. *MDM4* knockdown activated p53, induced cell cycle arrest, and decreased tumor growth in a xenograft model in a p53-dependent manner. Small molecule inhibition of the MDM4-p53 interaction was effective only in TP53wt BL cell lines. Moreover, primary TP53wt BL samples frequently acquired gains of chromosome 1q, which includes the *MDM4* locus, and showed elevated MDM4 mRNA levels. 1q gain was associated with TP53wt across 789 cancer cell lines and *MDM4* was essential in the TP53wt-context in 216 cell lines representing 19 cancer entities from the Achilles project. Our findings highlight the critical role of p53 as a tumor suppressor in BL and identify MDM4 as a functional target of 1q gain in a wide range of cancers that is therapeutically targetable.

Keywords

Burkitt lymphoma, RNAi, MDM4, 1q gain, TP53 mutation, MYC, MDM2, TCF3

Significance Statement

Author Manuscript Published OnlineFirst on April 18, 2019; DOI: 10.1158/0008-5472.CAN-18-3438
Author manuscripts have been peer reviewed and accepted for publication but have not yet been edited.

Targeting MDM4 to alleviate degradation of p53 can be exploited therapeutically across Burkitt Lymphoma and other cancers with wild-type p53 harboring 1q gain, the most frequent copy number alteration in cancer.

Introduction

Burkitt lymphoma (BL) is an aggressive B cell lymphoma that is characterized by translocation of the *MYC* gene to immunoglobulin loci (1). While oncogenic MYC promotes cell growth and proliferation, it also evokes failsafe mechanisms such as p53 activation that have to be overcome for transformation (2). About 40% of BL acquire *TP53* mutations evading MYC-induced stress signals (3,4).

Recent mutational cartography efforts in BL identified additional recurrent mutations in *TCF3*, *ID3*, *GNA13*, *RET*, *PIK3R1*, *DDX3X*, *FBXO11*, and the SWI/SNF genes *ARID1A* and *SMARCA4* (5-8). BL also display copy number alterations (CNAs) in addition to the *MYC* translocation, targeting chromosomes 1q, 13q31, 17p13 (including *TP53*) and 9p21.2 (including *CDKN2A*) (9,10). A gain of 1q is found in 30% of BL and often affects large regions (11), which has contributed to the limited understanding of oncogenic mechanisms involved. The implications of these mutations and CNAs are currently unclear.

RNAi-based genomics screens allow querying of functional dependencies in an unbiased fashion and in high-throughput. Using panels of representative cell lines, context-specific vulnerabilities have been linked to genetic and pathological subgroups (12). The Achilles Project reported comprehensive screening data in 501 cell lines using RNAi (13,14). While activating mutations caused direct oncogene addiction, as seen in cell lines with *BRAF*, *KRAS* or *PI3K* mutation, secondary gene dependencies were observed for loss-of-function mutations in tumor suppressor genes, such as *ARID1A* (15). Integration of gene expression and drug sensitivity profiles may provide further insight into the molecular basis of diseases and might be used to tailor targeted therapies (16).

Author Manuscript Published OnlineFirst on April 18, 2019; DOI: 10.1158/0008-5472.CAN-18-3438
Author manuscripts have been peer reviewed and accepted for publication but have not yet been edited.

For a comprehensive dissection of molecular dependencies in BL, we performed a loss-of-function RNAi screen across a panel of genetically characterized BL cell lines and intersected our findings on genotype-specific essential genes with the genetic profile of a well-annotated patient cohort.

Author Manuscript Published OnlineFirst on April 18, 2019; DOI: 10.1158/0008-5472.CAN-18-3438
Author manuscripts have been peer reviewed and accepted for publication but have not yet been edited.

Methods

Raw shRNA read counts from the RNAi screen and scripts used for processing are available upon request.

Microarray data are available at ArrayExpress under the accession number E-MTAB-7134.

Supplemental methods and tables are available with the online version of this article.

Cell culture. BJAB, BL-2, CA46, Namalwa, Ramos, Raji, BL-41, DogKit, DG-75 and Gumbus were obtained from DSMZ (Braunschweig, Germany), BL7, BL60, LY47 were provided by G.M. Lenoir (IARC, Lyon, France), Salina, Seraphine, and Cheptanges were provided by A. Rickinson, (Birmingham, UK) and 293T/17 by Stefan Fröhling (DKFZ, Heidelberg, Germany). All cell lines were maintained under standard conditions. Cell line authentification was performed using Multiplex Cell Authentification and cell cultures were tested for contamination and mycoplasma using the Cell Contamination Test (Multiplexion, Heidelberg, Germany).

RNAi screen and shRNA-mediated knock-down

The RNAi screen was performed as described previously (17) with modifications using the DECIPHER™ Human Module I pooled lentiviral shRNA library (#DHPAC-M1-P) targeting 5,045 genes in key signaling pathways with 4-5 shRNAs per gene (Cellecta, Mountain View, CA, USA). shRNA representation was determined two and 14 days post-transduction using high-throughput sequencing. p-values for shRNA depletion were calculated using the edgeR package (18) and collapsed into gene scores using weighted Z-transformation (19). p-values for differential shRNA viability effects were calculated as described previously using public software and collapsed into gene scores using Kolmogorov-Smirnov statistics (https://software.broadinstitute.org/GENE-E/index.html). RNAi results in non-BL cell lines screened with the same library were provided by Cellecta as raw read counts and genome-wide RNAi results in 216 cell lines were publically available as log2-transformed shRNA fold-changes (13). Single shRNAs were co-expressed with RFP constitutively from the pRSI12-U6-(sh)-UbiC-TagRFP-2A-Puro vector backbone. shRNA cytotoxicity was determined by transduction of 50% of cells and relative RFP-loss compared to a scrambled shRNA (shNT).

Genetic annotation of cell lines

Mutations in BL cell lines were identified from genomic DNA using a self-designed amplicon panel (20) or from RNA sequencing on the Illumina HiSeq2000. Sequences were mapped against the human reference genome hg19 using the STAR alignment tool. Mutations were called as described previously (21).

Author Manuscript Published OnlineFirst on April 18, 2019; DOI: 10.1158/0008-5472.CAN-18-3438
Author manuscripts have been peer reviewed and accepted for publication but have not yet been edited.

Genetic information for non-BL cell lines was extracted from CCLE (https://portals.broadinstitute.org/ccle/home) and COSMIC (GDSC, http://www.cancerrxgene.org/).

RT-qPCR

Total RNA was isolated with RNeasy Mini Kit (Qiagen) and on-column DNase I (Qiagen) digestion. RNA was reverse-transcribed by Super-Script III First-Strand Synthesis Supermix (Invitrogen) and quantified using QuantiFast SYBR Green RT-PCR (Qiagen) or Power SYBR Green Master Mix (Applied Biosystems) on a LightCycler 480 Real-Time PCR System, software v1.5 (Roche Applied Sciences).

Immunoblotting

Antibodies were from Merck Millipore (anti-MDM4 04-1555; anti-MDM2 OP46), abcam (anti-GAPDH, ab9485), BD Pharmingen (anti-p53 554294), Cell Signaling (anti-cleaved PARP 9546; anti-mouse IgG DyLight800 5257; anti-rabbit IgG (H+L) DyLight680 5366), or Santa Cruz (anti-p21 556431; anti-PUMA sc-28226). The LI-COR Odyssey Infrared Imaging System (Cell Signaling) was used for detection and Image J (National Institutes of Health, Bethesda, MA, USA) for band quantification.

CRISPR/Cas9 gene knock-out

sgRNAs were co-expressed with Cas9 from lentiCRISPRv2 (Addgene, Cambridge, MA, USA, plasmid #52961). Seraphine cells with effective p53 knock-out were selected using puromycin and Nutlin-3.

Cell cycle analysis

Cells were incubated for 2h with BrdU and analyzed in flow cytometry using anti-BrdU-APC and 7-AAD from the BrdU Flow Kit (552598, BD Pharmingen).

Gene expression profiling

Total RNA of cell cultures with > 80% shRNA+/RFP+ cells was hybridized on a Illumina BeadChip HumanHT-12-v4 containing >47,000 probes for 31,000 annotated human genes. Gene Set Enrichment Analysis (GSEA) was performed for C2 and H gene sets from the MSigDB database using software provided by the BroadInstitut (http://software.broadinstitute.org/gsea/msigdb) (22).

Xenograft model

Animal studies were performed in agreement with the Guide for Care and Use of Laboratory Animals published by the US National Institutes of Health (NIH Publication n. 85–23, revised 1996), in compliance with the German law on the protection of animals, and with the approval of the regional authorities responsible (Regierung von Oberbayern). The *in vivo* experiments were performed as published

Author Manuscript Published OnlineFirst on April 18, 2019; DOI: 10.1158/0008-5472.CAN-18-3438
Author manuscripts have been peer reviewed and accepted for publication but have not yet been edited.

previously (23). Briefly, Seraphine-TP53wt, Seraphine-TP53ko and Raji cell lines were infected *in vitro* with shNT or shMDM4 aiming at >80% transduction efficiency. 1x10^7 cells were subcutaneously injected into flanks of immunodeficient mice. Tumor growth was monitored by FDG-PET after 11 or 16 days depending on the graft efficiency and mice were sacrificed.

ATP-based growth assay

Cell content of DMSO and drug-treated cells was determined by ATP level after 48h incubation using CellTiter-Glo luminescent assay (Promega, Madison, WI, USA) as described (24). After normalization to DMSO, IC_{50} values were calculated with GraphPad Prism using nonlinear regression to fit the data to the log(inhibitor) vs. response (variable slope) curve as described in the manual of the software.

Genetic profile of primary BL patients

Copy number alterations were analyzed by CGH using a BAC/PAC array consisting of 2799 DNA fragments as described elsewhere (25,26) and by SNP array (GSE21597). Interphase FISH analysis was performed on paraffin-embedded or frozen tissue sections to determine *MYC*, *BCL2* and *BCL6* translocations to IG regions. *TP53* mutations were determined by DHPLC and sequencing of exons 4-10 of the coding region (27). The expression data of primary samples was downloaded from Gene Expression Omnibus (http://www.ncbi.nlm.nih.gov/geo, GSE43677). Patients were classified into BL, DLBCL and an intermediate group based on a previously described molecular signature (28). For all samples, tumor cell content exceeded 70%. The study was performed as part of the "Molecular Mechanisms in Malignant Lymphomas" Network Project of the Deutsche Krebshilfe and was approved by a central ethics commission (University Hospital, Göttingen). Written informed consent was obtained in accordance with the Declaration of Helsinki.

Author Manuscript Published OnlineFirst on April 18, 2019; DOI: 10.1158/0008-5472.CAN-18-3438
Author manuscripts have been peer reviewed and accepted for publication but have not yet been edited.

Results

Landscape of essential genes in BL

To identify therapeutic targets in BL, we investigated molecular dependencies in BL cell lines using RNAi-based loss-of-function screening. We used a pooled shRNA library to silence 5,045 genes including members of signal transduction pathways, drug targets and disease-associated genes with 4-5 shRNAs per gene and assessed changes in shRNA abundance after culturing the cells for two weeks (Figure 1A). On average 24% of shRNAs were depleted at least two-fold and shRNAs targeting core essential complexes, including the ribosome and the proteasome, were specifically lost (68% and 47%, respectively) (Figure 1B). To evaluate the viability effect of individual gene knock-downs, we calculated weighted z-scores that combine the effect of shRNAs targeting the same gene and emphasize strong fold-changes (18,19). Common essential genes, as defined on the basis of previous RNAi screens (29), showed significantly lower scores compared to non-essential genes ($p<0.001$, Figure 1C). Notably, while a subset of genes was essential in all cell lines, we also observed cell line specific viability effects (Figure S1A).

To investigate essential genes in the context of BL, we probed our data against RNAi screening results using the same set of shRNAs in six carcinoma cell lines (C4-2, DU145, PC3, R22v1, MDA-MB-231, A2780) and three cell lines of myeloid and lymphoid origin (AML193, THP1, U937) (Figure S1B). We ranked shRNAs based on their differential effects between two cell line groups and calculated a gene classification score as a measurement of their strength to distinguish between the groups (12) (Table S1). We then selected genes that were predictors of an entity group and showed strong differential viability effects based on the weighted z-scores. To exclude core essential genes, gene scores in eight BL cell lines were first compared to the six carcinomas. We identified 76 genes essential in BL, including genes associated with hematopoietic cell differentiation (*FLI1*, *BCL11A*) or B cell development and

Author Manuscript Published OnlineFirst on April 18, 2019; DOI: 10.1158/0008-5472.CAN-18-3438
Author manuscripts have been peer reviewed and accepted for publication but have not yet been edited.

activation (*PAX5*, *CDKN1B*, *JAK2*, *CARD11*) (Figure 1D, *left*). We therefore investigated, if these viability genes were classifiers of BL or of the blood lineage (Figure S1C). Knock-down of *FLI1,* a transcriptional regulator of the hematopoietic system and B cell development (30), was also toxic to blood-lineage derived non-BL cell lines, while *PAX5*, a marker of early B-cell development, was an essential gene exclusively in BL (Figure 1D, *middle*/*right*).

Genotype-specific dependencies in BL

We next investigated essential genes in the context of a specific gene mutation. We performed RNA sequencing of the BL cell lines included in the RNAi screen, and compared essential genes in the respective genotype groups focusing on genes that are recurrently mutated in BL, such as *TP53*, *ID3*, *TCF3*, *DDX3X*, *FOXO1* and *GNA13* (5-8) (Table S2). Mutations in the transcription factor *TCF3* lead to oncogene activation and loss-of-function mutations of its inhibitor *ID3* are often observed as a complementary mechanism of TCF3 activation (7). Therefore, cell lines carrying either *TCF3* or *ID3* mutation were treated as one group. The four cell lines with *TCF3*/*ID3* mutation were strongly dependent on TCF3 expression, indicating oncogene addiction ($p<0.01$) (Figure 1E). In line with the loss of function effect of mutations in *ID3*, ID3 silencing was not toxic (Figure 1E, *left*). The cell line BL2 harbors the activating p.S219C mutation in MYD88, an adaptor protein involved in Toll-Like-Receptor signaling and NF-kB activation. shRNAs targeting *MYD88* or its direct downstream mediator *IRAK1* were specifically toxic in the MYD88mut context (Figure 1F). Encouraged by the ability to uncover oncogene addiction, we expanded our analysis of genotype-specific vulnerabilities to *DDX3X*, *FOXO1*, *GNA13* and *TP53* (Table S1; Figure S1D). *TP53* mutation was associated with the strongest differential viability effects (gene classification scores >2, Table S1) and we therefore focused on *TP53*-specific vulnerabilities.

Author Manuscript Published OnlineFirst on April 18, 2019; DOI: 10.1158/0008-5472.CAN-18-3438
Author manuscripts have been peer reviewed and accepted for publication but have not yet been edited.

p53 pathway susceptibilities in BL

We identified seven genes (*MDM4*, *CDKN3*, *BRCA2*, *BHMT2*, *SRC*, *PPP2R1A*, *PPM1D*) that were essential in TP53wt BL cell lines (Figure 2A). Notably, as Epstein-Barr virus (EBV) associated proteins deregulate cell cycle checkpoints and quench the p53 pathway by deubiquitination of the p53 inhibitor MDM2 (31), we confirmed a balanced distribution of EBV infection status among TP53wt and TP53mut BL cell lines (Table S2). To test the p53-specificity in a larger set of cell lines, we analyzed gene effect scores in 19 TP53wt and 42 TP53mut cell lines of hematopoietic/lymphoid origin from a combined RNAi screen of the DepMap project (14) (Figure 2B). All candidate genes showed a trend towards lower gene effect scores in TP53wt cell lines. We did not identify robust vulnerabilities for the mutant p53 context (Figure 2A, S2). Genes with a significantly lower effect score in TP53mut cell lines of the DepMap project, were associated with the TP53 pathway and portrayed a growth advantage to TP53wt cell lines (Figure S2A-D).

We chose the two most robust hits, *MDM4* and *CDKN3*, for validation experiments. *CDKN3* is a spindle checkpoint phosphatase essential for G1-S transition during the cell cycle (32). shRNAs targeting *CDKN3* efficiently reduced *CDKN3* mRNA level (Figure 2C). Using two non-overlapping shRNAs, we tested the screen findings in a growth competition assay in five TP53wt and seven TP53mut BL cell lines. shRNAs were co-expressed with red fluorescent protein (RFP) in ~50% of cells and the fraction of RFP+/shRNA+ cells was monitored over time. The knock-down of *CDKN3* was toxic to 4/5 TP53wt cell lines (Figure 2D). To further test whether the observed effects were dependent on p53, we generated a p53 knock-out cell line based on the TP53wt cell line Seraphine (Figure S3A). The toxicity of *CDKN3* knock-down was partially rescued with one shRNA in Seraphine-TP53ko (Figure 2D).

MDM4 inactivates p53-mediated transcription by blocking of its transactivation domain (33). shRNAs targeting MDM4 efficiently reduced MDM4 mRNA and protein levels (Figure 2E). The knock-down was

Author Manuscript Published OnlineFirst on April 18, 2019; DOI: 10.1158/0008-5472.CAN-18-3438
Author manuscripts have been peer reviewed and accepted for publication but have not yet been edited.

toxic in 3/4 TP53wt cell lines, but not in seven TP53mut BL cell lines, and the effect was completely rescued in isogenic Seraphine-TP53ko with one shRNA and partially rescued with a second shRNA (Figure 2F). The BL2 cell lines that was less responsive to *CDKN3* and *MDM4* knock-down carries a deletion of the *CDKN2A* locus encoding for p53 activator p14 and p16 and shows a lower basal p53 pathway activity, which might explain the milder effect (Figure S3B).

MDM4 promotes cell cycle progression by p53 inactivation

To understand the downstream effects of MDM4 depletion in BL, we assessed protein levels of p53 and known p53 targets. MDM4 knock-down in TP53wt cells increased p53 protein level and induced the pro-apoptotic Bcl-2 family member PUMA and the cell cycle inhibitor p21 (Figure 3A). Since MDM4 downregulation did not cause apoptosis as determined by absence of PARP cleavage (Figure 3A), we analyzed the cell cycle profile in the presence or absence of functional p53 after MDM4 silencing. In the TP53wt context, shRNAs targeting MDM4 decreased cycling cells compared to a non-targeting shRNA (shNT, $p<0.001$), which was not observed in the TP53mut cell line Raji and rescued in the Seraphine-TP53ko cell line (Figure 3B). Further cell cycle profiling in additional cell lines confirmed p53-specific induction of cell cycle arrest following MDM4 knock-down (Figure S3C).

We next determined global gene expression changes after MDM4 and MDM2 silencing in the TP53wt and TP53ko Seraphine cell lines (Figure 3C, Table S3). Silencing of MDM4 or MDM2 induced strong changes only in the presence of p53 and affected similar pathways. Using gene set enrichment analysis for cancer hallmark genes (MSigDB), we identified p53 targets as the strongest upregulated pathway, while prominent survival and proliferation pathways, including MYC and E2F targets, were downregulated. This suggests that most effects were mediated by p53 activation, in accordance with a previous report on genes commonly regulated after MDM4 or MDM2 knock-down (34). We also compared genes differentially regulated by MDM2 or MDM4 silencing (Figure S4). Downregulation of

Author Manuscript Published OnlineFirst on April 18, 2019; DOI: 10.1158/0008-5472.CAN-18-3438
Author manuscripts have been peer reviewed and accepted for publication but have not yet been edited.

MYC and upregulation of *CCND1* were exclusively seen after MDM4 knock-down, indicating potential differences in pathway contribution exerted by MDM4 over MDM2.

We next examined the basal protein and mRNA expression levels of p53, MDM4 and MDM2 in a panel of BL models (Figure 3D). p53 protein was detected at higher level in all TP53mut cell lines ($p<0.01$) as described previously (35), while p53 mRNA levels were lower ($p=0.045$). Wild-type p53 is rapidly turned-over in a negative feed-back loop mediated by MDM2 and mutant p53 protein accumulates as a result of disrupted proteasomal decay (36). MDM4 mRNA was significantly higher in TP53wt BL cell lines ($p=0.027$) and was correlated with protein expression ($p<0.01$) (Figure 3D).

MDM4 is a therapeutic target in TP53wt BL

To evaluate the potential of MDM4 as a therapeutic target in TP53wt BL *in vivo*, we determined the effect of MDM4 silencing on tumor growth in a mouse xenograft model. After transduction, cell lines representing TP53wt (Seraphine), TP53ko (Seraphine-TP53ko) and TP53mut (Raji) were injected subcutaneously into the flanks of immunodeficient mice (23). To quantify tumor formation and dynamic growth, we measured fludeoxyglucose (FDG) uptake in positron emission tomography (PET). *In vivo* tumor formation was significantly reduced after MDM4 knockdown in the presence of wild-type p53 ($p<0.05$) (Figure 4A, B).

Restoration of p53 activity is an attractive therapeutic approach for treatment of cancer (37). The small molecule inhibitor Nutlin-3 is targeting the p53 inhibitor MDM2 and therefore restores signaling through the p53 pathway (38). TP53wt BL cell lines were sensitive towards Nutlin-3 with an average IC_{50} value of 4µM, while the average IC_{50} for TP53mut cell lines was 27µM. The reduction in cell numbers was significantly stronger in TP53wt cell lines starting from a concentration of 1.11µM (1.11µM: p=0.016 *, 3.33µM: p=1.60e-04 ***, 10µM: p=2.98e-06 ***, 30µM: p=1.86e-03 **) (Figure 4C). We tested the specificity of Nutlin-3 in the isogenic cell lines Seraphine-TP53wt and Seraphine-TP53ko and observed an

Author Manuscript Published OnlineFirst on April 18, 2019; DOI: 10.1158/0008-5472.CAN-18-3438
Author manuscripts have been peer reviewed and accepted for publication but have not yet been edited.

increase of p53 levels in the TP53wt cell line (Figure S3A) and p53-dependent induction of apoptosis using 10µM Nutlin-3 (Figure S3D).

Despite the high sequence homology of MDM2 and MDM4, Nutlin-3 targets MDM2 with a much higher binding affinity (39). Moreover, overexpression of MDM4 can lead to resistance against MDM2-targeting drugs (39). We therefore tested the dual-specificity inhibitor RO-5963, that targets MDM2 and MDM4 (40), and observed a higher sensitivity in TP53wt BL cell lines starting at a concentration of 1.11µM (1.11µM: p=0.017 *, 3.33µM: p=0.0014 **, 10µM: p=0.002 **) (Figure 4D). The average IC_{50} in TP53wt cell lines was 4.6µM. The highest concentration tested was 10µM and IC_{50} was not reached for most TP53mut cell lines. This data provides a rational for targeting MDM4/2 in TP53wt BL.

Gain of MDM4 on chr1q provides an alternative to *TP53* mutations in BL

To understand the role of the p53 pathway in BL, we analyzed the genetic profile of aggressive B-cell lymphoma patients classified into BL, diffuse large B cell lymphoma (DLBCL) or cases with intermediate phenotype (28) (Table S4). *TP53* mutations were found in 28/61 (45.9%) of BL samples and were significantly more frequent in BL than in DLBCL (p<0.001) (Figure 5A). *MYC* box I mutations were previously reported to be mutually exclusive with *TP53* mutations and to serve as an alternative mechanism to escape apoptotic pathways in the presence of wild-type *TP53* (4). *MYC* mutations were present in 37/56 BL samples (66.1%) and the *MYC* box I residues 56-58 were affected in 20 (35.7%) cases (Figure 5B). Notably, *MYC* box I mutations frequently co-occurred with *TP53* mutations (Figure 5B).

We next explored the profile of copy number alterations (CNAs) in Burkitt lymphoma stratified by *TP53* mutation status (Figure 5C). The most frequent gains were on 1q21-q23 (TP53wt: 39%/TP53mut: 20%), 1q24-q25 (32%/8%), 1q32.1 (29%/12%), 2p16.1 (23%/20%), 11q12.3-q13.1 (13%/20%), 6p22 (14.3%) and 3q27.3 (29%/36%%), and the most frequent loss was on 17p13 (4%/20%). Deletion of 17p13 included the *TP53* gene and co-occurred with *TP53* mutation in 5/6 cases resulting in bi-allelic p53

Author Manuscript Published OnlineFirst on April 18, 2019; DOI: 10.1158/0008-5472.CAN-18-3438
Author manuscripts have been peer reviewed and accepted for publication but have not yet been edited.

inactivation. Notably, loss of the MDM2 inhibitor ARF (*CDKN2A* locus on 9p21.3), that has been described as an alternative mechanism of p53 inactivation in BL cell lines (41), was rare in primary BL biopsies (n=1). Chr1q gain was the most frequent CNA in TP53wt BL, which was not seen in DLBCL (Figure S5A) or intermediated cases (Figure S5B), and besides of 1q21, chromosomal gains frequently affected 1q32, including the MDM4 locus (Figure 5D).

As 1q gain affected a large region with further oncogenes, we tested if BL cell lines from the RNAi screen were more dependent on genes on 1q (Figure 5E, F). The RNAi library covered 235 genes located on 1q including known oncogenes. All four TP53wt BL cell lines were previously reported to carry a 1q gain (42). In Seraphine, the whole chromosomal arm was affected (+1q21.1qter), while partial gains were seen in BL-2 (+1q21.1q31.3), LY47 (+1q43q44), and Seraphine (+1q21.1qter). The TP53mut cell lines were diploid for 1q (Table S2). Genes on 1q were not enriched for viability genes in the group of TP53wt or TP53mut BL cell lines, respectively (Figure 5E). Notably, *MDM4* was the only gene showing *TP53*-specific viability effects after silencing (Figure 5F).

Altogether, our data support a critical role for quenching of the p53 pathway in BL preferably by mutations of *TP53* or amplification of *MDM4*, thereby identifying p53 signaling as the critical failsafe checkpoint in BL.

_TP53_ mutations and MDM4 gain inactivate the p53 pathway in primary BL

To study the functional consequences of p53 pathway aberrations, we generated a molecular signature that distinguished TP53wt and TP53mut B-cell non-Hodgkin-Lymphoma (B-NHL, n=430) using supervised hierarchical clustering (Figure 6A). The gene *CDKN2A* was significantly repressed in TP53wt BL ($p<0.01$), intermediate lymphoma ($p<0.01$) and DLBCL ($p<0.01$) samples (Figure 6B). Within the 50 most differentially expressed gene probes with lower expression in TP53mut patients, 28 were located on chr17p13 and 4 gene probes were located on chr1q (Figure 6A). These findings reflect the gene dosage

Author Manuscript Published OnlineFirst on April 18, 2019; DOI: 10.1158/0008-5472.CAN-18-3438
Author manuscripts have been peer reviewed and accepted for publication but have not yet been edited.

effect as a result of chr17p13 deletion in TP53mut and chr1q gain in TP53wt patients. Nine probes corresponding to six p53 target genes were expressed in TP53wt samples, demonstrating that a portion of aggressive B-NHL retain active p53 signaling. Therefore, elevated *MDM2* levels in TP53wt DLBCL ($p<0.01$) and BL ($p<0.01$) might be a consequence of a p53 activity (Figure 6C). Notably, high MDM4 mRNA expression was specific to BL with TP53wt ($p<0.01$, Figure 6D). MDM4 expression was high in all BL with chr1q gain, but also in some TP53wt BL without 1q gain, indicating that additional mechanisms regulate MDM4 expression (Figure S6). Combined, these data provide evidence for upregulation of MDM4 in TP53wt BL as a disease driver.

MDM4 and _TP53_ mutation across cancer models

To investigate the role of chr1q gain in context of *TP53* mutations across a range of cancer types, we analyzed the associations between genetic aberrations in 789 cell lines with available SNP6.0 data and *TP53* mutation data within the Cancer Cell Line Encyclopedia (43). Chr1q32 gain was identified in 122 cell lines (15.5%) and was associated with wild-type p53 ($p<0.001$, 23% in TP53wt and 12% in TP53mut) (Figure 7A). We further combined genetic information with functional genomics data and investigated p53-dependent vulnerabilities in a set of 216 cell lines representing 19 cancer entities from the Achilles project (13). *TP53* and chr1q32 status were available for 182 cell lines. *TP53* mutations were present in 70% of all cancer cell lines and chr1q32 was also significantly associated with TP53wt ($p<0.001$) (Figure 7B, Table S5). Notably, *MDM4* was the top ranked gene leading to impaired viability of TP53wt cell lines out of more than 10,000 genes investigated ($p<0.001$) (Figure 7C, Table S6). All shRNAs targeting *MDM4* were strongly depleted in TP53wt cell lines (Figure 7D). MDM2 also showed significant shRNA depletion in TP53wt cell lines ($p=0.004$, rank 51, Figure 7C).

Eight cancer entities were represented with at least two TP53mut and two TP53wt cell lines which allowed us to explore *MDM4* dependency in different cancer subtypes (Figure 7E, Table S6). We observed entity-specific preference for MDM4 over MDM2: *MDM4* was identified as an essential gene

Author Manuscript Published OnlineFirst on April 18, 2019; DOI: 10.1158/0008-5472.CAN-18-3438
Author manuscripts have been peer reviewed and accepted for publication but have not yet been edited.

in TP53wt cell lines derived from the hematopoietic/lymphoid system (rank 1), large intestine (rank 3), breast carcinoma (rank 25) and ovarian carcinoma (rank 62) (Figure 7F). p53-specific dependency on MDM2 were strongest in ovarian carcinoma (rank 20) and CNS (rank 8) (Figure 7F).

Combined these data suggest a functional role for MDM4 as a critical cancer driver targeted by 1q gain across cancers.

Author Manuscript Published OnlineFirst on April 18, 2019; DOI: 10.1158/0008-5472.CAN-18-3438
Author manuscripts have been peer reviewed and accepted for publication but have not yet been edited.

Discussion

The combination of sequencing efforts and functional genomics serves as a powerful tool to understand the pathogenesis of diseases and to discover molecular targets. This study dissected specific vulnerabilities in BL using RNAi screening. We observed a strong dependency of BL on PAX5, a key B-cell transcription factor previously linked to B-cell lymphomagenesis (44), in accordance to a genome-wide CRISPR/Cas9 screen in two BL cell lines (45). These findings identify PAX5 as a "lineage-survival oncogene" (46)and demonstrate the power of genetic perturbation screens in dissection of "non-oncogene addictions" (47) that may not be predicted from the genetic profile. The increased capacity to drug transcription factors (48) as well as the recent demonstration of the role of PAX5 as a metabolic gatekeeper (49) suggests that PAX5 targeting may provide a novel therapeutic strategy.

Previously, a RNAi interference screen using a targeted shRNA library was used to characterize the B-cell receptor pathway in BL cell lines (7). This study also revealed gene mutation specific dependencies and found BL lines rely on cyclin D3/CDK6 for cell cycle progression and cyclin D3 mutants augment this effect. We add to these data by systematically querying genotype-specific vulnerabilities of BL. We identified oncogene dependency on TCF3 in *TCF3/ID3* mutant BL, and dependency on MYD88 and IRAK1 in a cell line with *MYD88* mutation, consistent with previous results in BL and DLBCL (7,50). The strongest dependency was observed for MDM4 in TP53wt cell lines and further underscores the importance of suppressing p53-mediated stress signals in the pathogenesis of BL with activation of the *MYC* oncogene. Reactivation of p53 by inhibition of MDM4 is a promising therapeutic approach in melanoma (51) and breast carcinomas (52). We validated MDM4 as a potential target in TP53wt BL using a mouse xenograft model and showed effective p53-specific cytotoxicity for MDM2/MDM4 dual inhibition.

Author Manuscript Published OnlineFirst on April 18, 2019; DOI: 10.1158/0008-5472.CAN-18-3438
Author manuscripts have been peer reviewed and accepted for publication but have not yet been edited.

Chromosome 1q gain is the most frequent copy number across cancer (53), but functional evidence for the disease drivers affected by 1q gain has been lacking. Cytogenetic studies in BL identified gains for 1q25.1 and 1q31.3 and suggested *PTPRC*, a regulator of B-cell receptor and cytokine signaling, and two annotated miRNA genes (hsa-mir-181b-1 and -213) as strong candidates (9). A study of primary tumors and cell lines identified *BCA2* and *PIAS3* on 1q21.-1q21.3, *MDM4* on 1q32.1 and *AKT3* on 1q44 as possible drivers (42). In an unbiased approach, we now identified an association of 1q gain with wild-type p53 in primary BL, a finding not observed for DLBCL. While DLBCL develops diverse mechanisms of p53 and cell cycle deregulation (54), our genetic perturbation screen provides functional evidence that 1q gain and *TP53* mutation are specifically selected for in BL to inactivate p53 activity. A pan-cancer analysis also revealed entity-specific dependency on MDM4 in TP53wt cancer cells with important clinical implications for p53 reactivating compounds.

MDM2 and MDM4 have been reported to be frequently deregulated in cancer (reviewed in Eischen and Lozano 2014 (55)). We identified entity-specific preferences for MDM4 or MDM2 dependency. Our data suggest that among lymphomas, BL exhibits disease specific mechanisms of p53 pathway suppression via *TP53* mutation and MDM4 overexpression. A major open question pertains to the selective advantage of MDM4 or MDM2 overexpression in TP53wt cancers. MDM4 and MDM2 are highly homologous and closely interact to regulate the p53 pathway (55). In addition, p53-independent oncogenic activities were described for both proteins. MDM4, for example, was shown to promote pRb degradation by MDM2 and therefore enhances cell cycle progression by E2F1 activation (56). In our study, we identified downregulation of *MYC* and upregulation of *CCND1* after MDM4, but not MDM2 knock-down, indicating differences in pathway contribution exerted by MDM4 over MDM2 that need further exploration.

Author Manuscript Published OnlineFirst on April 18, 2019; DOI: 10.1158/0008-5472.CAN-18-3438
Author manuscripts have been peer reviewed and accepted for publication but have not yet been edited.

MDM2 overexpression by enhanced translation was described in TP53wt BL cell lines (41). In pediatric BL (pBL), that shows p53 mutations at a lower frequency than adult BL, MDM2 overexpression and p53 mutation accounted for 55% of cases (57). MDM4 mRNA was shown to be overexpressed in TP53wt pBL, some of which harbored a 1q gain (58). Our results extend these findings in adult BL.

Oncogenic MYC activation provokes p53-mediated apoptosis (2) and MYC-induced lymphomagenesis in transgenic mice is dependent on secondary lesions that promote survival (59). Mutations in the conserved *Myc* box I were shown to prevent the induction of apoptosis via Bim in a mouse xenograft model and to occur mutually exclusively to *TP53* mutations in primary BL samples (4). In our study, however, *TP53* mutations occurred independent of *MYC* box I mutations.

Based on the incidence of *TP53* mutation and 1q gain in the disease, our findings suggest a widespread mechanism to suppress p53 activity in BL to overcome p53-mediated cell cycle arrest and apoptosis caused by MYC overexpression. This provides critical biological and therapeutic rationale for targeting MDM4 in *TP53* wild-type diseases.

Acknowledgements

The work was supported by the *Helmholtz Virtual Institute* „Understanding and overcoming resistance to apoptosis and therapy in leukemia", the Helmholtz initiative *iMed* on Personalized Medicine, the European Union (FP7 projects *Radiant, Systems Microscopy*, Horizon 2020 project *SOUND*) and the "Monique Dornonville de la Cour – Stiftung".

The "Deutsche Krebshilfe" supported TZ ("Mildred-Scheel" Professorship), ML ("Mildred-Scheel" Fellowship), the Monique-Dornonville de la Cour Stiftung and the "Molecular Mechanisms of Malignant Lymphoma – MMML" consortium. RS/RW received infrastructural support by the "KinderKrebsInitiative Buchholz Holm-Seppensen".

We thank the microarray unit of the DKFZ Genomics and Proteomics Core Facility for providing the Illumina Whole-Genome Expression Beadchips and related services, and the high-throughput sequencing unit for providing RNA sequencing services. We thank Hanno Glimm, Stefan Fröhling, Daniela Richter, Roland Eils, Peter Lichter, Stephan Wolf, Katja Beck and Janna Kirchhof for infrastructure and program development within DKFZ-HIPO and NCT POP, and Tina Uhrig for technical assistance and Agnes Hotz-Wagenblatt for shRNA alignment. We thank Anna Jauch for FISH analysis in BL cell lines. We thank Henry-Jacques Delecluse and Astrid Hofmann for staining of EBV proteins in BL cell lines to determine the EBV status and latency phase.

References

1. Dalla-Favera R, Bregni M, Erikson J, Patterson D, Gallo RC, Croce CM. Human c-myc onc gene is located on the region of chromosome 8 that is translocated in Burkitt lymphoma cells. Proceedings of the National Academy of Sciences of the United States of America 1982;79(24):7824-7.
2. Hermeking H, Eick D. Mediation of c-Myc-induced apoptosis by p53. Science 1994;265(5181):2091-3.
3. Gaidano G, Ballerini P, Gong JZ, Inghirami G, Neri A, Newcomb EW, et al. p53 mutations in human lymphoid malignancies: association with Burkitt lymphoma and chronic lymphocytic leukemia. Proceedings of the National Academy of Sciences of the United States of America 1991;88(12):5413-7.
4. Hemann MT, Bric A, Teruya-Feldstein J, Herbst A, Nilsson JA, Cordon-Cardo C, et al. Evasion of the p53 tumour surveillance network by tumour-derived MYC mutants. Nature 2005;436(7052):807-11.
5. Love C, Sun Z, Jima D, Li G, Zhang J, Miles R, et al. The genetic landscape of mutations in Burkitt lymphoma. Nature genetics 2012.
6. Richter J, Schlesner M, Hoffmann S, Kreuz M, Leich E, Burkhardt B, et al. Recurrent mutation of the ID3 gene in Burkitt lymphoma identified by integrated genome, exome and transcriptome sequencing. Nature genetics 2012.
7. Schmitz R, Young RM, Ceribelli M, Jhavar S, Xiao W, Zhang M, et al. Burkitt lymphoma pathogenesis and therapeutic targets from structural and functional genomics. Nature 2012;490(7418):116-20.
8. Kretzmer H, Bernhart SH, Wang W, Haake A, Weniger MA, Bergmann AK, et al. DNA methylome analysis in Burkitt and follicular lymphomas identifies differentially methylated regions linked to somatic mutation and transcriptional control. Nature genetics 2015;47(11):1316-25.
9. Scholtysik R, Kreuz M, Klapper W, Burkhardt B, Feller AC, Hummel M, et al. Detection of genomic aberrations in molecularly defined Burkitt's lymphoma by array-based, high resolution, single nucleotide polymorphism analysis. Haematologica 2010;95(12):2047-55.
10. Schiffman JD, Lorimer PD, Rodic V, Jahromi MS, Downie JM, Bayerl MG, et al. Genome wide copy number analysis of paediatric Burkitt lymphoma using formalin-fixed tissues reveals a subset with gain of chromosome 13q and corresponding miRNA over expression. British journal of haematology 2011;155(4):477-86.
11. Salaverria I, Zettl A, Bea S, Hartmann EM, Dave SS, Wright GW, et al. Chromosomal alterations detected by comparative genomic hybridization in subgroups of gene expression-defined Burkitt's lymphoma. Haematologica 2008;93(9):1327-34.
12. Cheung HW, Cowley GS, Weir BA, Boehm JS, Rusin S, Scott JA, et al. Systematic investigation of genetic vulnerabilities across cancer cell lines reveals lineage-specific dependencies in ovarian cancer. Proceedings of the National Academy of Sciences of the United States of America 2011;108(30):12372-7.
13. Cowley GS, Weir BA, Vazquez F, Tamayo P, Scott JA, Rusin S, et al. Parallel genome-scale loss of function screens in 216 cancer cell lines for the identification of context-specific genetic dependencies. Scientific data 2014;1:140035.
14. Tsherniak A, Vazquez F, Montgomery PG, Weir BA, Kryukov G, Cowley GS, et al. Defining a Cancer Dependency Map. Cell 2017;170(3):564-76 e16.
15. Helming KC, Wang X, Wilson BG, Vazquez F, Haswell JR, Manchester HE, et al. ARID1B is a specific vulnerability in ARID1A-mutant cancers. Nature medicine 2014;20(3):251-4.

16. Marcotte R, Sayad A, Brown KR, Sanchez-Garcia F, Reimand J, Haider M, et al. Functional Genomic Landscape of Human Breast Cancer Drivers, Vulnerabilities, and Resistance. Cell 2016;164(1-2):293-309.
17. Slabicki M, Lee KS, Jethwa A, Sellner L, Sacco F, Walther T, et al. Dissection of CD20 regulation in lymphoma using RNAi. Leukemia 2016;30(12):2409-12.
18. Dai Z, Sheridan JM, Gearing LJ, Moore DL, Su S, Dickins RA, et al. shRNA-seq data analysis with edgeR. F1000Res 2014;3:95.
19. Kim J, Tan AC. BiNGS!SL-seq: A Bioinformatics Pipeline for the Analysis and Interpretation of Deep Sequencing Genome-Wide Synthetic Lethal Screen. Next Generation Microarray Bioinformatics: Methods and Protocols 2012;802:389-98.
20. Hullein J, Jethwa A, Stolz T, Blume C, Sellner L, Sill M, et al. Next-generation sequencing of cancer consensus genes in lymphoma. Leuk Lymphoma 2013;54(8):1831-5.
21. International Cancer Genome Consortium PedBrain Tumor P. Recurrent MET fusion genes represent a drug target in pediatric glioblastoma. Nature medicine 2016;22(11):1314-20.
22. Subramanian A, Tamayo P, Mootha VK, Mukherjee S, Ebert BL, Gillette MA, et al. Gene set enrichment analysis: a knowledge-based approach for interpreting genome-wide expression profiles. Proceedings of the National Academy of Sciences of the United States of America 2005;102(43):15545-50.
23. Herhaus P, Habringer S, Philipp-Abbrederis K, Vag T, Gerngross C, Schottelius M, et al. Targeted positron emission tomography imaging of CXCR4 expression in patients with acute myeloid leukemia. Haematologica 2016;101(8):932-40.
24. Dietrich S, Oles M, Lu J, Sellner L, Anders S, Velten B, et al. Drug-perturbation-based stratification of blood cancer. The Journal of clinical investigation 2018;128(1):427-45.
25. Schwaenen C, Nessling M, Wessendorf S, Salvi T, Wrobel G, Radlwimmer B, et al. Automated array-based genomic profiling in chronic lymphocytic leukemia: development of a clinical tool and discovery of recurrent genomic alterations. Proceedings of the National Academy of Sciences of the United States of America 2004;101(4):1039-44.
26. Fiegler H, Carr P, Douglas EJ, Burford DC, Hunt S, Scott CE, et al. DNA microarrays for comparative genomic hybridization based on DOP-PCR amplification of BAC and PAC clones. Genes, chromosomes & cancer 2003;36(4):361-74.
27. Zenz T, Eichhorst B, Busch R, Denzel T, Habe S, Winkler D, et al. TP53 mutation and survival in chronic lymphocytic leukemia. Journal of clinical oncology : official journal of the American Society of Clinical Oncology 2010;28(29):4473-9.
28. Hummel M, Bentink S, Berger H, Klapper W, Wessendorf S, Barth TF, et al. A biologic definition of Burkitt's lymphoma from transcriptional and genomic profiling. N Engl J Med 2006;354(23):2419-30.
29. Hart T, Brown KR, Sircoulomb F, Rottapel R, Moffat J. Measuring error rates in genomic perturbation screens: gold standards for human functional genomics. Molecular systems biology 2014;10:733.
30. Zhang XK, Moussa O, LaRue A, Bradshaw S, Molano I, Spyropoulos DD, et al. The transcription factor Fli-1 modulates marginal zone and follicular B cell development in mice. Journal of immunology 2008;181(3):1644-54.
31. Saha A, Murakami M, Kumar P, Bajaj B, Sims K, Robertson ES. Epstein-Barr virus nuclear antigen 3C augments Mdm2-mediated p53 ubiquitination and degradation by deubiquitinating Mdm2. Journal of virology 2009;83(9):4652-69.
32. Nalepa G, Barnholtz-Sloan J, Enzor R, Dey D, He Y, Gehlhausen JR, et al. The tumor suppressor CDKN3 controls mitosis. The Journal of cell biology 2013;201(7):997-1012.

33. Shvarts A, Bazuine M, Dekker P, Ramos YF, Steegenga WT, Merckx G, et al. Isolation and identification of the human homolog of a new p53-binding protein, Mdmx. Genomics 1997;43(1):34-42.
34. Heminger K, Markey M, Mpagi M, Berberich SJ. Alterations in gene expression and sensitivity to genotoxic stress following HdmX or Hdm2 knockdown in human tumor cells harboring wild-type p53. Aging (Albany NY) 2009;1(1):89-108.
35. Farrell PJ, Allan GJ, Shanahan F, Vousden KH, Crook T. p53 is frequently mutated in Burkitt's lymphoma cell lines. The EMBO journal 1991;10(10):2879-87.
36. Vijayakumaran R, Tan KH, Miranda PJ, Haupt S, Haupt Y. Regulation of Mutant p53 Protein Expression. Frontiers in oncology 2015;5:284.
37. Burgess A, Chia KM, Haupt S, Thomas D, Haupt Y, Lim E. Clinical Overview of MDM2/X-Targeted Therapies. Frontiers in oncology 2016;6:7.
38. Vassilev LT, Vu BT, Graves B, Carvajal D, Podlaski F, Filipovic Z, et al. In vivo activation of the p53 pathway by small-molecule antagonists of MDM2. Science 2004;303(5659):844-8.
39. Patton JT, Mayo LD, Singhi AD, Gudkov AV, Stark GR, Jackson MW. Levels of HdmX expression dictate the sensitivity of normal and transformed cells to Nutlin-3. Cancer Res 2006;66(6):3169-76.
40. Graves B, Thompson T, Xia M, Janson C, Lukacs C, Deo D, et al. Activation of the p53 pathway by small-molecule-induced MDM2 and MDMX dimerization. Proceedings of the National Academy of Sciences of the United States of America 2012;109(29):11788-93.
41. Lindstrom MS, Klangby U, Wiman KG. p14ARF homozygous deletion or MDM2 overexpression in Burkitt lymphoma lines carrying wild type p53. Oncogene 2001;20(17):2171-7.
42. Toujani S, Dessen P, Ithzar N, Danglot G, Richon C, Vassetzky Y, et al. High resolution genome-wide analysis of chromosomal alterations in Burkitt's lymphoma. PloS one 2009;4(9):e7089.
43. Barretina J, Caponigro G, Stransky N, Venkatesan K, Margolin AA, Kim S, et al. The Cancer Cell Line Encyclopedia enables predictive modelling of anticancer drug sensitivity. Nature 2012;483(7391):603-7.
44. Cozma D, Yu D, Hodawadekar S, Azvolinsky A, Grande S, Tobias JW, et al. B cell activator PAX5 promotes lymphomagenesis through stimulation of B cell receptor signaling. The Journal of clinical investigation 2007;117(9):2602-10.
45. Wang T, Birsoy K, Hughes NW, Krupczak KM, Post Y, Wei JJ, et al. Identification and characterization of essential genes in the human genome. Science 2015.
46. Garraway LA, Sellers WR. Lineage dependency and lineage-survival oncogenes in human cancer. Nature reviews Cancer 2006;6(8):593-602.
47. Solimini NL, Luo J, Elledge SJ. Non-oncogene addiction and the stress phenotype of cancer cells. Cell 2007;130(6):986-8.
48. Filippakopoulos P, Qi J, Picaud S, Shen Y, Smith WB, Fedorov O, et al. Selective inhibition of BET bromodomains. Nature 2010;468(7327):1067-73.
49. Chan LN, Chen Z, Braas D, Lee JW, Xiao G, Geng H, et al. Metabolic gatekeeper function of B-lymphoid transcription factors. Nature 2017;542(7642):479-83.
50. Ngo VN, Young RM, Schmitz R, Jhavar S, Xiao W, Lim KH, et al. Oncogenically active MYD88 mutations in human lymphoma. Nature 2011;470(7332):115-9.
51. Gembarska A, Luciani F, Fedele C, Russell EA, Dewaele M, Villar S, et al. MDM4 is a key therapeutic target in cutaneous melanoma. Nature medicine 2012.
52. Haupt S, Buckley D, Pang JM, Panimaya J, Paul PJ, Gamell C, et al. Targeting Mdmx to treat breast cancers with wild-type p53. Cell death & disease 2015;6:e1821.
53. Beroukhim R, Mermel CH, Porter D, Wei G, Raychaudhuri S, Donovan J, et al. The landscape of somatic copy-number alteration across human cancers. Nature 2010;463(7283):899-905.

54. Monti S, Chapuy B, Takeyama K, Rodig SJ, Hao Y, Yeda KT, et al. Integrative analysis reveals an outcome-associated and targetable pattern of p53 and cell cycle deregulation in diffuse large B cell lymphoma. Cancer cell 2012;22(3):359-72.
55. Eischen CM, Lozano G. The Mdm network and its regulation of p53 activities: a rheostat of cancer risk. Hum Mutat 2014;35(6):728-37.
56. Zhang H, Hu L, Qiu W, Deng T, Zhang Y, Bergholz J, et al. MDMX exerts its oncogenic activity via suppression of retinoblastoma protein. Oncogene 2015;34(44):5560-9.
57. Wilda M, Bruch J, Harder L, Rawer D, Reiter A, Borkhardt A, et al. Inactivation of the ARF-MDM-2-p53 pathway in sporadic Burkitt's lymphoma in children. Leukemia 2004;18(3):584-8.
58. Leventaki V, Rodic V, Tripp SR, Bayerl MG, Perkins SL, Barnette P, et al. TP53 pathway analysis in paediatric Burkitt lymphoma reveals increased MDM4 expression as the only TP53 pathway abnormality detected in a subset of cases. British journal of haematology 2012;158(6):763-71.
59. Sander S, Calado DP, Srinivasan L, Kochert K, Zhang B, Rosolowski M, et al. Synergy between PI3K signaling and MYC in Burkitt lymphomagenesis. Cancer cell 2012;22(2):167-79.
60. Futreal PA, Coin L, Marshall M, Down T, Hubbard T, Wooster R, et al. A census of human cancer genes. Nature reviews Cancer 2004;4(3):177-83.

Author Manuscript Published OnlineFirst on April 18, 2019; DOI: 10.1158/0008-5472.CAN-18-3438
Author manuscripts have been peer reviewed and accepted for publication but have not yet been edited.

Figure legends

Figure 1. RNAi screening reveals context-specific vulnerabilities in BL.

(A) Layout of the RNAi screen in eight BL cell lines. Pooled shRNAs were tranduced lentivirally and shRNA abundance was determined by high-throughput sequencing. shRNAs interfering with survival or proliferation were lost over time. **(B)** shRNA depletion after two weeks of culture for all shRNAs (top) and shRNAs targeting the ribosome (middle) or proteasome (bottom). shRNAs with a fold-change of 2 or lower are marked in red, indicating specific depletion of shRNAs targeting core cellular complexes. **(C)** Weighted z gene viability scores (wZ) for common essential genes (n=73) and non-essential genes (n=149). **(D)** Comparison of essential genes in eight BL (orange) and six solid cancer cell lines (MDA-MB-231, A2780, C4-2, R22v1, PC3, DU-145) (blue). The volcano plot shows differences in wZ-scores and the rectangles mark the cut-off values at a p-value of 0.05 and difference of mean wZ-score of 1. The strongest lineage classifiers are labeled and shown in the heatmap that includes two AML (yellow) and one DLBCL (green) cell line to differentiate between BL- and hematopoietic/lymphoid -lineage classifiers. shRNA fold-changes are shown for *PAX5* (BL-lineage) and *FLI1* (hematopoietic/lymphoid -lineage). **(E)** Genetic dependencies in four BL cell lines with *TCF3* or *ID3* mutation and **(F)** one *MYD88* mutant cell line. shRNAs were ranked by their differential effects in BL2 (MYD88mut) and seven MYD88wt BL cell lines.

Figure 2. Gene dependencies in TP53wt BL.

(A) Difference in gene scores between four TP53wt and four TP53mut BL cell lines. Genes essential in TP53wt cell lines are marked and corresponding gene effect scores are shown on the right. **(B)** Gene effect scores in 19 TP53wt and 42 TP53mut cell lines of hematopoietic/lymphoid origin from the combined RNAi screen of the DepMap project for genes essential in TP53wt BL. **(C)** RT-qPCR for CDKN3 mRNA level three days after transduction of Seraphine-TP53ko. Expression values were normalized to

GAPDH and non-targeting shRNA. **(D)** Growth competition assay for two independent shRNAs targeting CDKN3. shRNAs were co-expressed with RFP in 50% of the cell culture. The fraction of shRNA+/RFP+ cells on day 14 post-transduction was normalized to day 3. Error bars show the mean standard error over TP53mut and TP53wt cell lines. **(E)** RT-qPCR and immunoblot for MDM4 level five days after transduction in BJAB and BL2, respectively. Expression values were normalized to GAPDH and non-targeting shRNA. Error bars indicate the mean with standard deviation of triplicate measurements (**: $p \leq 0.01$, ***: $p \leq 0.001$). **(F)** Growth competition assay following MDM4 knock-down as shown in figure **(D)**.

Figure 3. MDM4 depletion reactivates p53 and induces G1 arrest.

(A) Protein level of p53, p53 targets and apoptosis marker after MDM4 knock-down in Seraphine-p53wt. Cells were transduced with shRNAs, selected with puromycin and grown until day 5 before harvesting. Band intensities were normalized to GAPDH and shNT. **(B)** Cell cycle profile after MDM4 knock-down. Cells were transduced with shRNAs at >90% transduction efficiency and cultivated with BrdU for 2h. BrdU incorporation and total DNA content were measured by flow cytometry using a BrdU-APC conjugated antibody and 7-AAD, respectively. The plots show one representative measurement. Quantification of triplicate experiments is shown on the right (ns: $p \geq 0.05$, *: $p < 0.05$, ***: $p \leq 0.001$). **(C)** Global gene expression changes after MDM4 and MDM2 knock-down in isogenic Seraphine cell lines. Expression levels were normalized to shNT and gene set enrichment analysis was performed using the java-based GSEA software (http://software.broadinstitute.org/gsea/downloads.jsp (28,29)). Enrichment curves show the most enriched pathways and genes from these pathways are highlighted in blue (suppressed) or green (enriched), respectively. Genes highlighted in red were changed after MDM4, but not after MDM2 knock-down (cut-off –log10(p-value) > 2, log2(fold-change) < -0.5 or > 0.5). **(D)** Basal expression levels of MDM4, MDM2 and p53 in eight TP53wt (green) and eight TP53mut (red) BL cell

Author Manuscript Published OnlineFirst on April 18, 2019; DOI: 10.1158/0008-5472.CAN-18-3438
Author manuscripts have been peer reviewed and accepted for publication but have not yet been edited.

lines. Protein levels were measured in immunoblot and mRNA in RT-qPCR using GAPDH for normalization. The Pearson correlation between protein and mRNA level for p53 was R^2=0.3861 (p=0.10) in TP53wt and R^2=0.6557 (p=0.015) in TP53mut, and for R^2=0.8527 MDM4 in TP53wt (p=0.001) and R^2=0.2193 (p=0.24) in TP53mut. Differential mRNA expression of p53 (p=0.045) and MDM4 (p=0.027) is shown in boxplots.

Figure 4. MDM4 is a therapeutic target in TP53wt BL.

(A, B) MDM4 depletion reduces tumor growth in a mouse xenograft model. Indicated cell lines expressing shNT or shMDM4 were subcutaneously injected into the left (shNT) or right (shMDM4) flank of immunodeficient mice. **(A)** Exemplary images from FDG-PET analysis and quantification of FDG-uptake and **(B)** excised xenografts are shown. Error bars indicate mean of three mice per cell line and shRNA construct with standard error. **(C, D)** Cell line sensitivity towards chemical inhibition was measured by ATP content after 48h of incubation compared to DMSO. IC_{50} values are shown in brackets. **(C)** Ten TP53mut (red), seven TP53wt (green) and one TP53ko (blue) BL cell line were incubated with Nutlin-3. **(D)** Ten TP53mut (red) and eight TP53wt (green) BL cell lines were exposed to the dual MDM2/MDM4 inhibitor RO-5963.

Figure 5. Genetic aberrations frequently affect the p53 pathway in BL.

(A) Incidence of *TP53* mutations in BL (n=61), DLBCL (n=297) and the "intermediate" group (n=54) based on gene expression as determined by DHPLC and validation by Sanger sequencing. **(B)** Pattern of *TP53* mutations, *MYC* mutations and 1q gain in 61 BL. Each column represents a patient and the gene status is indicated as: red = mutation, beige = wild-type, white = missing data, dark red: mutations in MYC residues 56-58. **(C)** Genome-wide copy number alterations in TP53wt (n=31, left) and TP53mut (n=25, right) BL. Gains are shown in green and losses are shown in red. **(D)** Detailed mirror plots of the proportion of TP53mut (red) and TP53wt (green) BL patients with chromosome 1q gain by genomic

Author Manuscript Published OnlineFirst on April 18, 2019; DOI: 10.1158/0008-5472.CAN-18-3438
Author manuscripts have been peer reviewed and accepted for publication but have not yet been edited.

locus. Hallmark cancer consensus genes are indicated (60). **(E)** Mean weighted z-scores for genes on 1q (n=231) and genes not located on 1q (n=4,803) in four TP53wt (green) and four TP53mut (red) BL cell lines. **(F)** Mean weighted z-scores of four TP53wt and four TP53mut BL cell lines from the RNAi screen with indication of genes located on 1q and hallmark cancer consensus genes.

Figure 6. p53 pathway activation based on gene expression.

(A) Supervised hierarchical clustering of aggressive B-NHL patients (n=412) by molecular subtype and *TP53* mutation status using the 50 gene probes with higher (red) or lower (blue) expression in TP53mut samples. *TP53* status, 17p13 deletion and 1q gain are indicated above (black = aberration, grey = normal, white = not available). **(B-D)** Differential expression of CDKN2A **(B)**, MDM2 **(C)** and MDM4 **(D)** in lymphoma subtypes stratified by *TP53* mutation status.

Figure 7. MDM4 is essential in TP53wt cancers.

(A) Incidence of *TP53* mutation and chr1q32 gain in 789 cell lines. Information on the *TP53* status was available from COSMIC (Sanger Institute), CCLE (Broad-Novartis) and the IARC p53 data base. **(B)** Incidence of *TP53* mutation in cell lines of the Achilles project (version 2.4.3). Information on *TP53* mutation was available for 182 cell lines. **(C)** *TP53*-dependent essential genes across cancer cell lines. All genes were ranked based on their differential shRNA depletion in TP53wt (n=55) compared to TP53mut (n=127) cell lines. The genes on top of the ranking, including MDM4 and MDM2, were essential in TP53wt lines. Genes that do not target human genes (GFP, RFP, luciferase and Lac-Z) serve as non-essential control genes. **(D)** Depletion of shRNAs targeting MDM4 across all cell lines. The graph shows the fold-change in shRNA expression in TP53wt (green) and TP53mut (red) cell lines. **(E)** *TP53* mutation status for 216 cell lines from the Achilles Project by cancer entity. **(F)** Entity-specific analysis of TP53-dependent viability genes. Gene ranking was performed for all entities that had at least two cell lines per class as described for **(C)**.

Figure 1

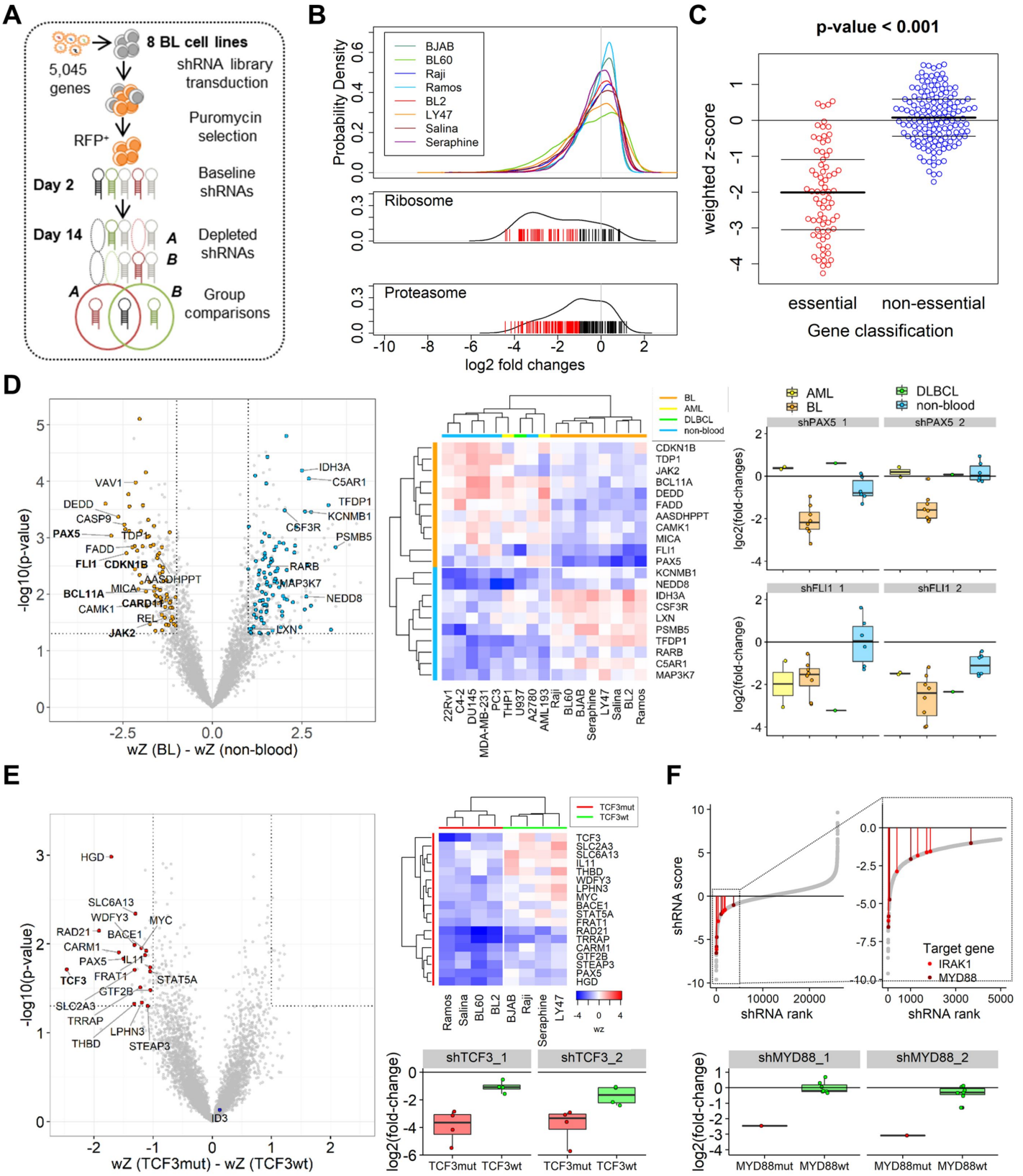

Figure 2

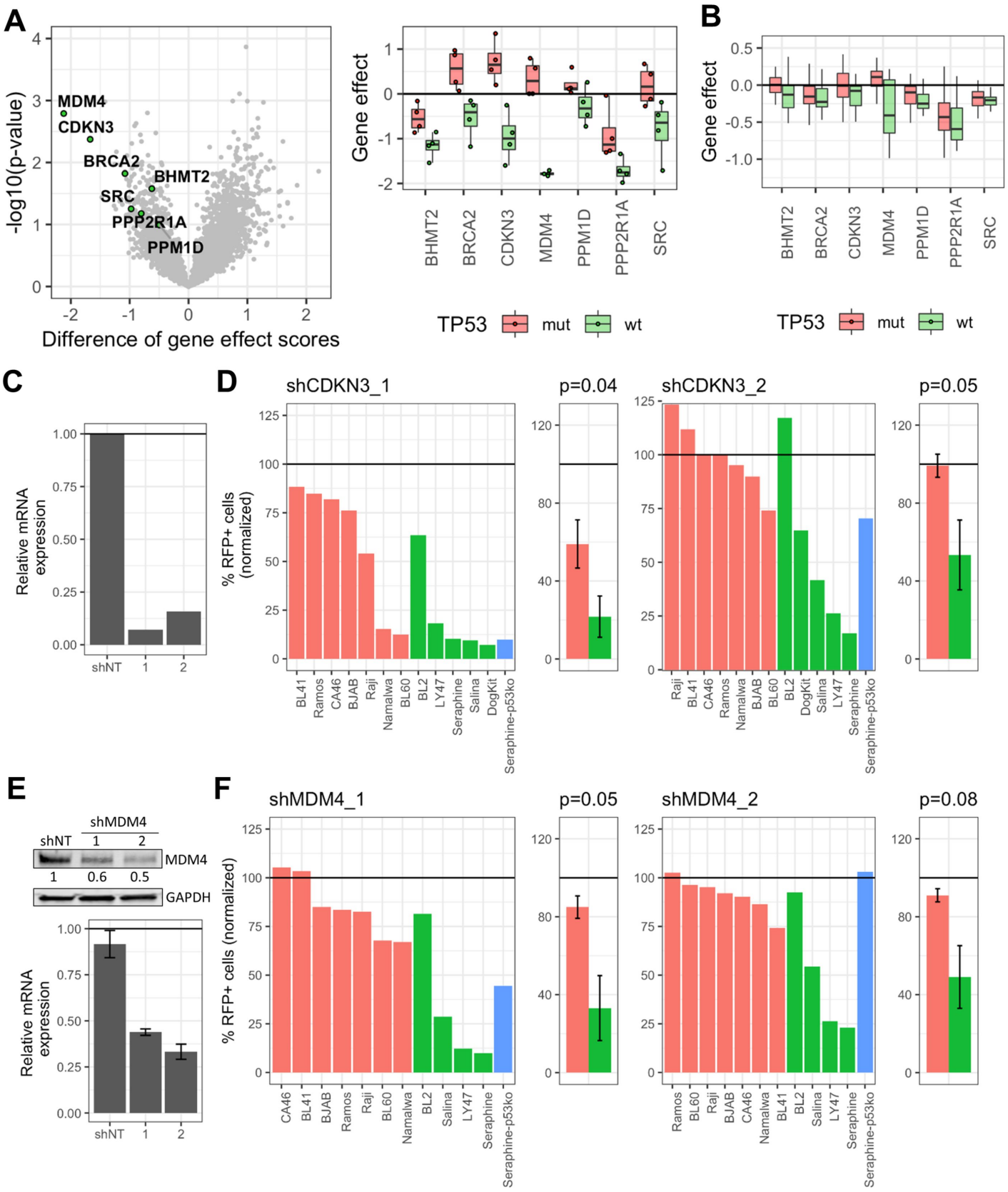

Figure 3

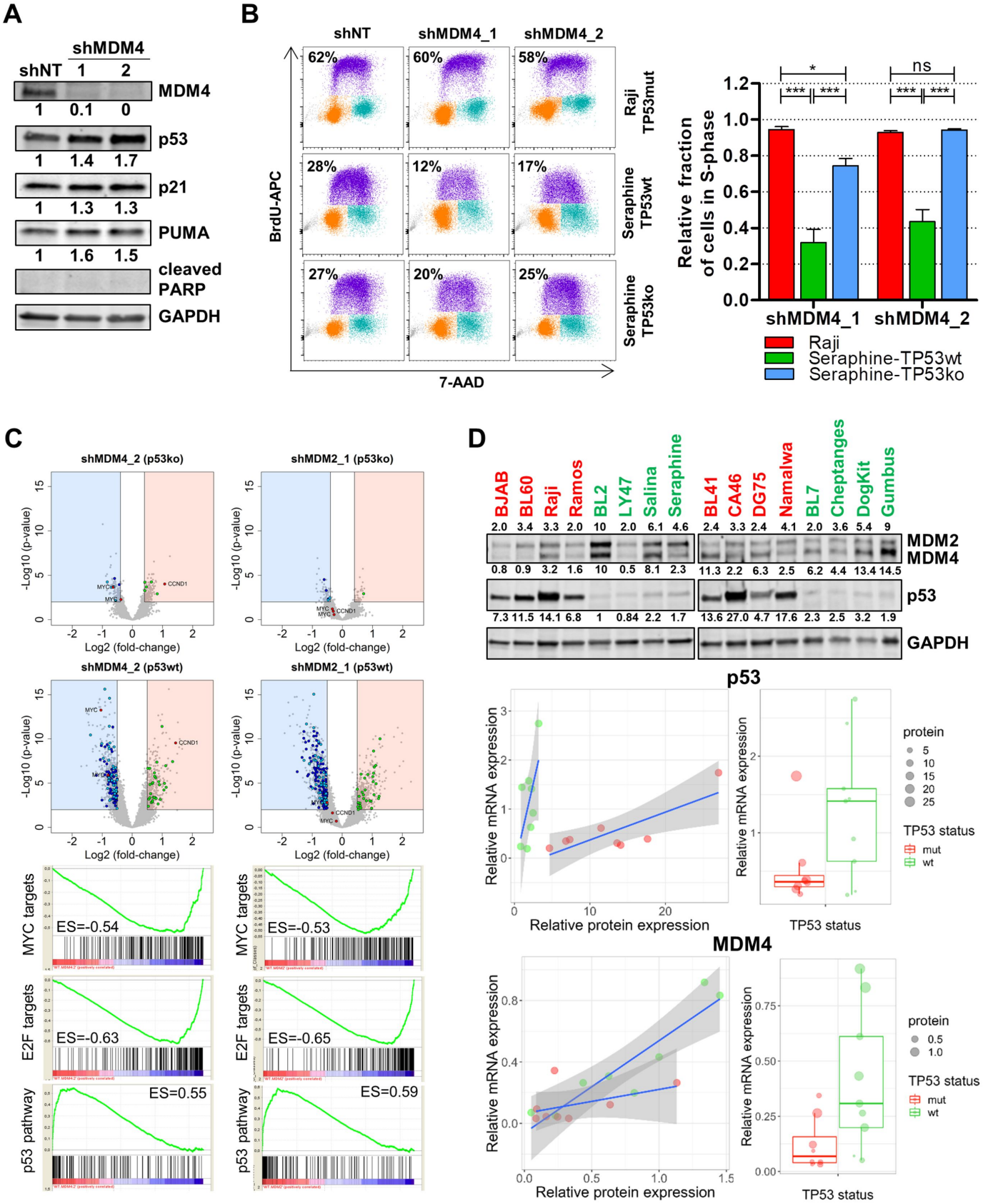

Figure 4

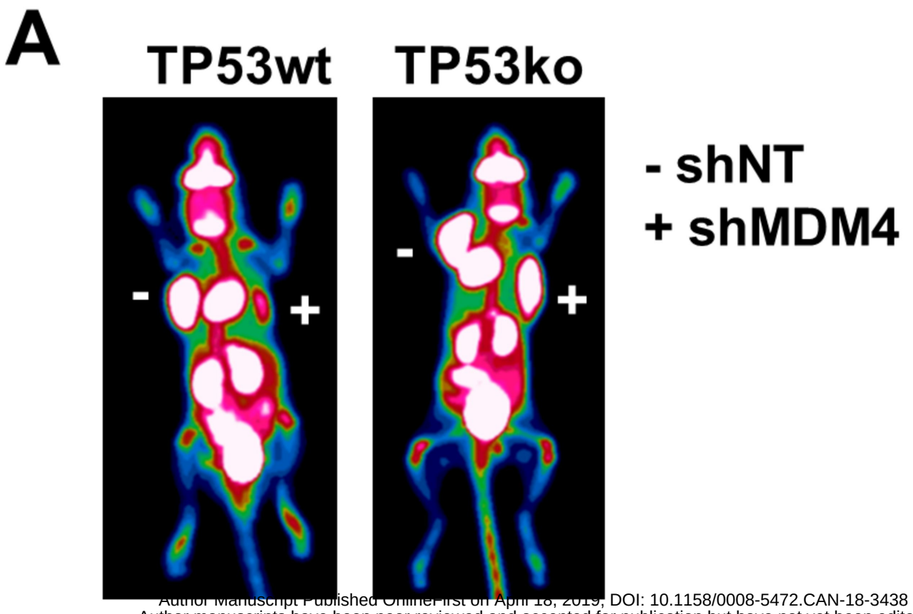

Author Manuscript Published OnlineFirst on April 18, 2019; DOI: 10.1158/0008-5472.CAN-18-3438
Author manuscripts have been peer reviewed and accepted for publication but have not yet been edited.

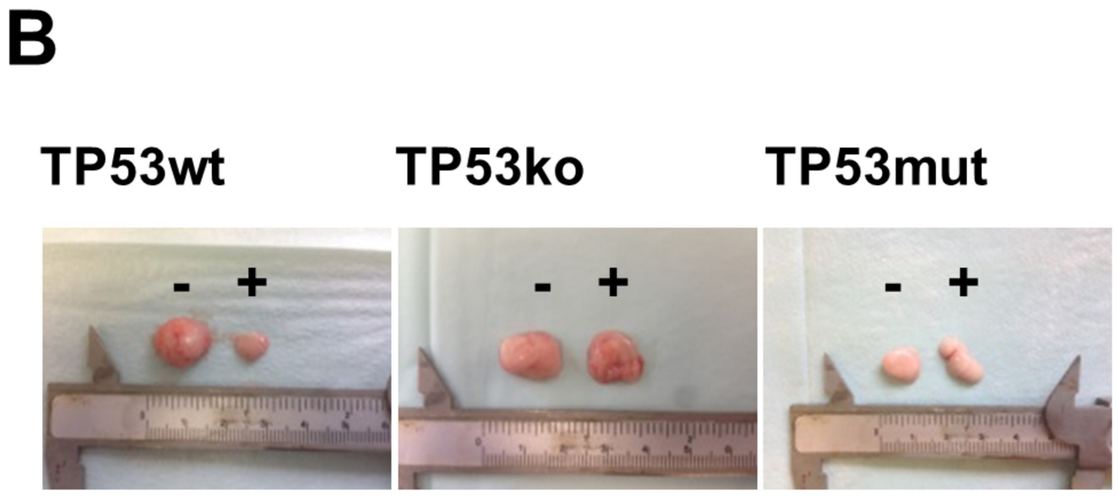

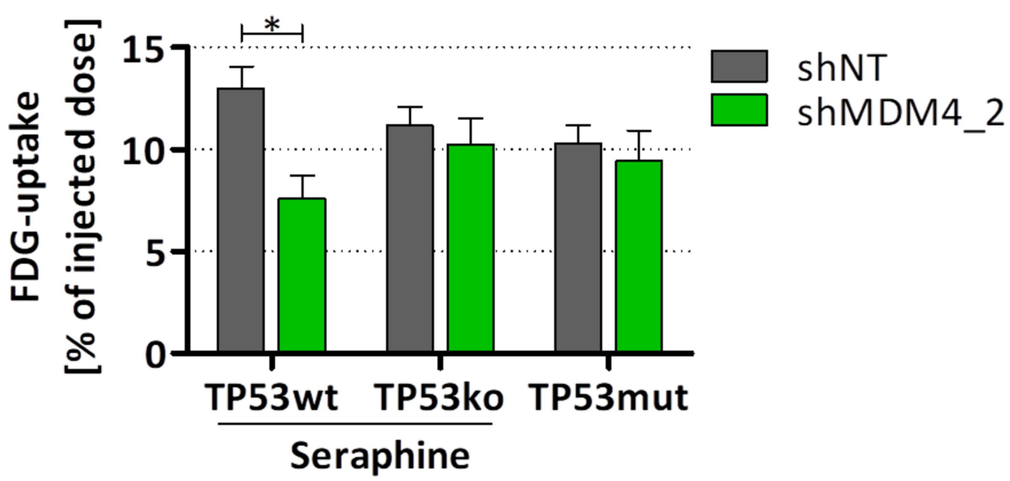

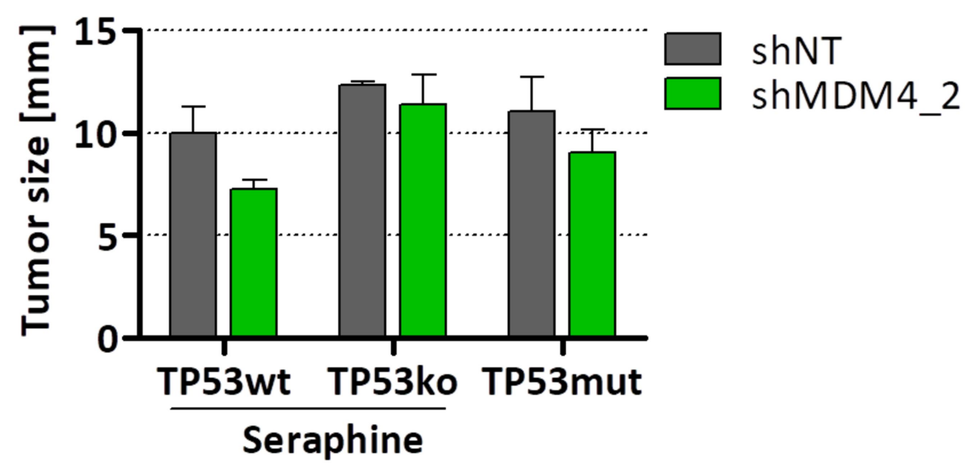

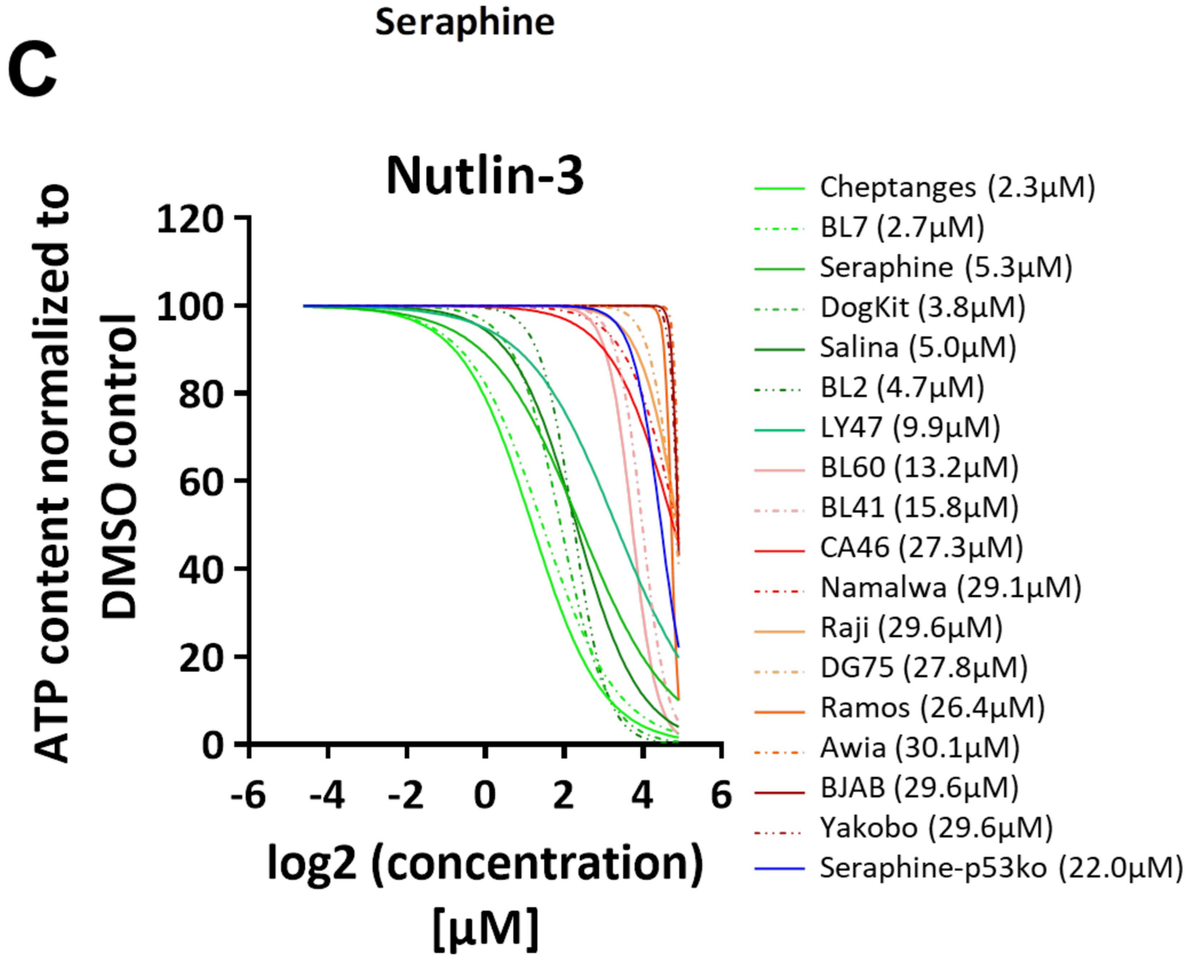

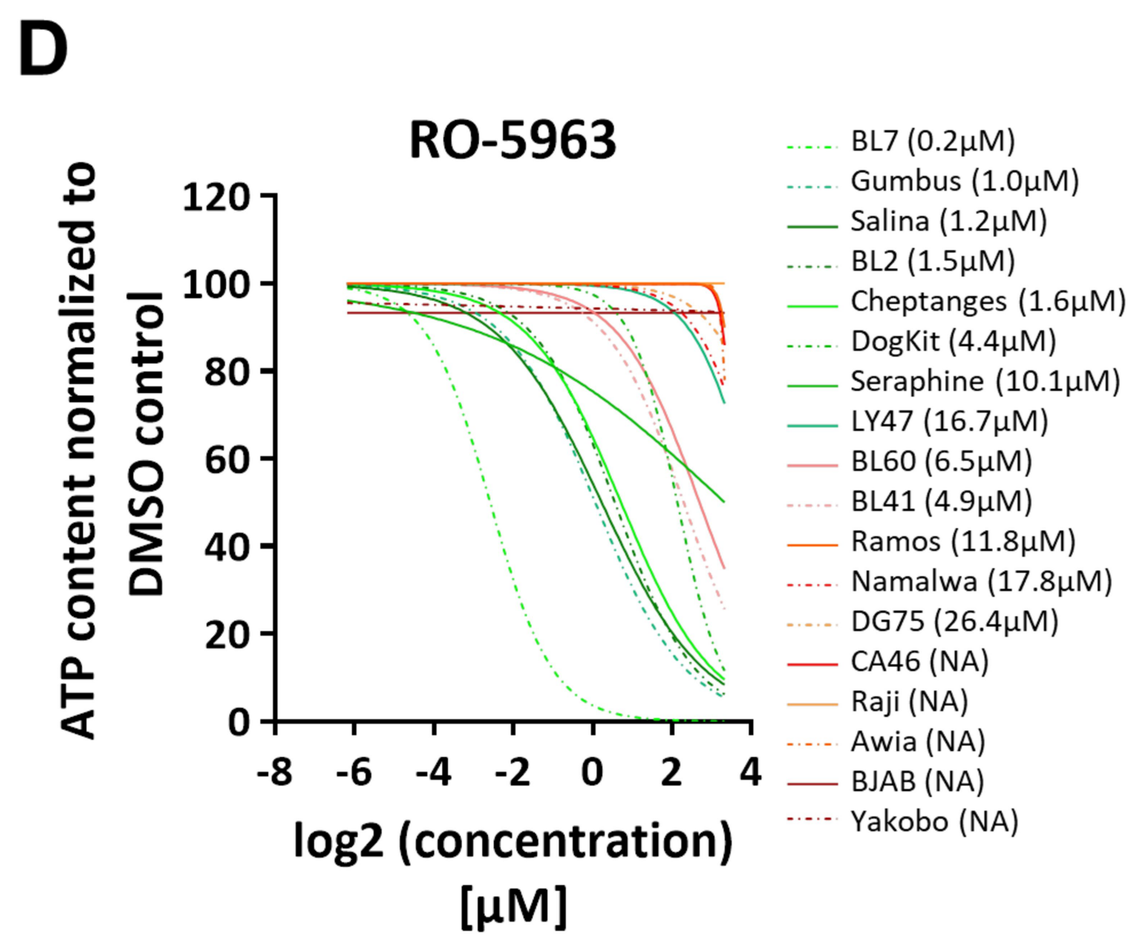

Figure 5

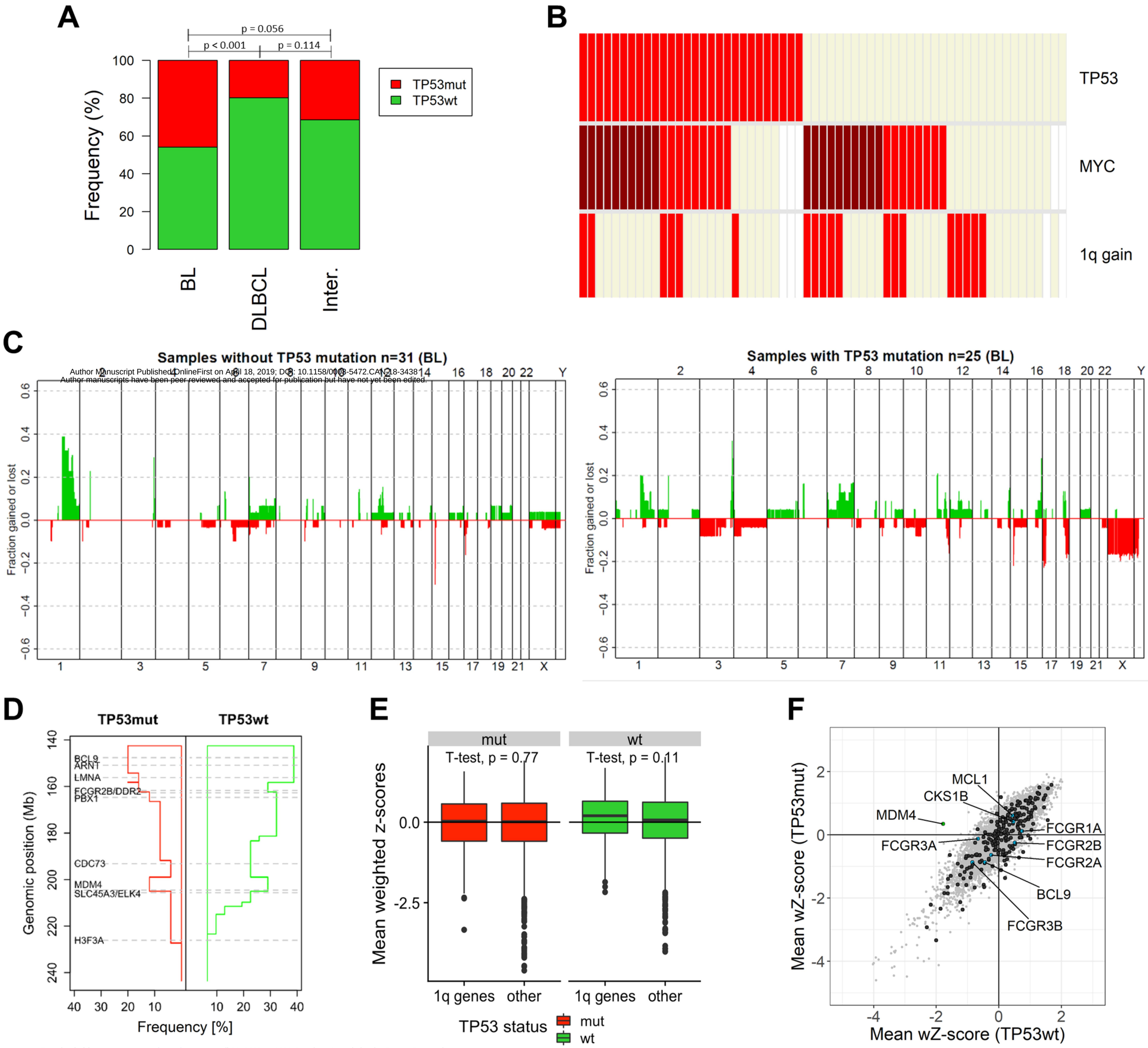

Author Manuscript Published OnlineFirst on April 18, 2019; DOI: 10.1158/0008-5472.CAN-18-3438
Author manuscripts have been peer reviewed and accepted for publication but have not yet been edited.

Figure 6

A

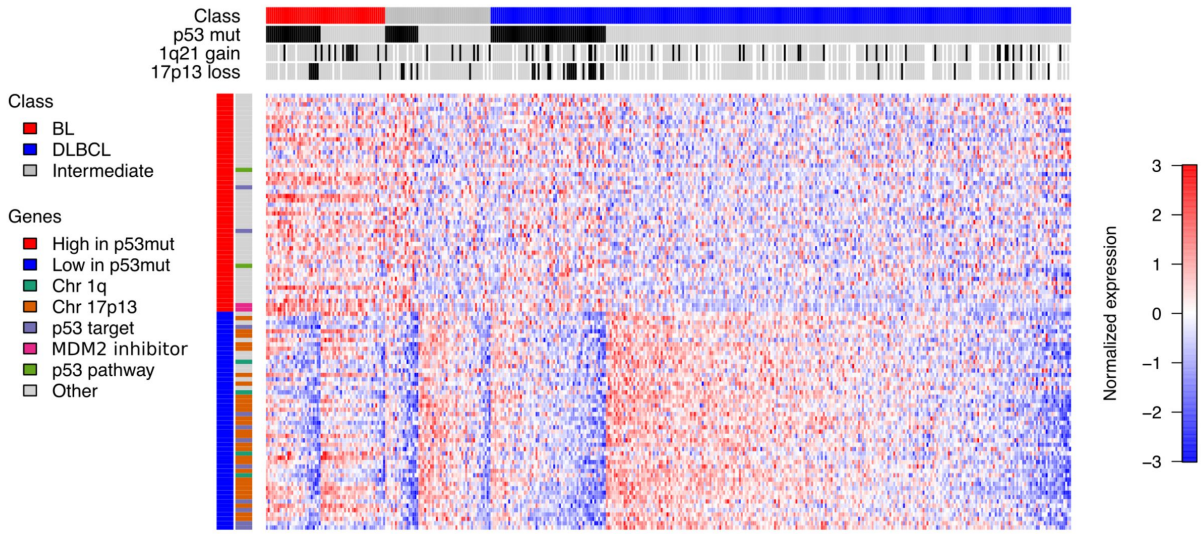

B

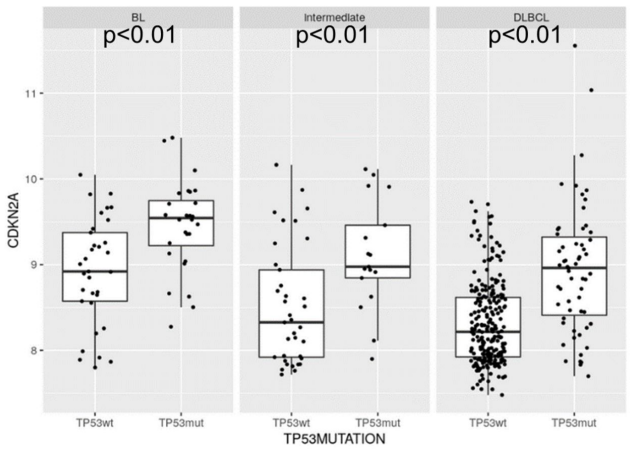

C

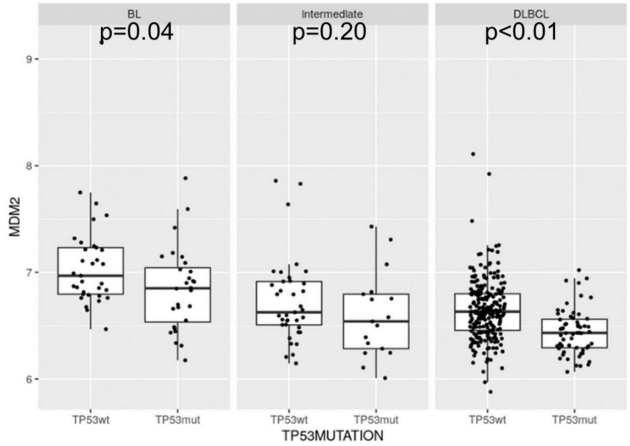

D

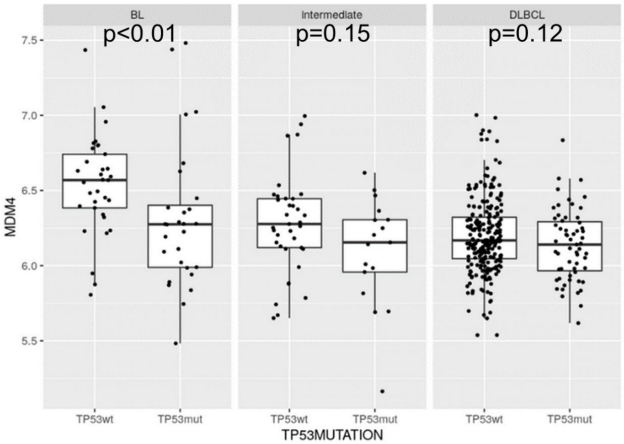

Figure 7

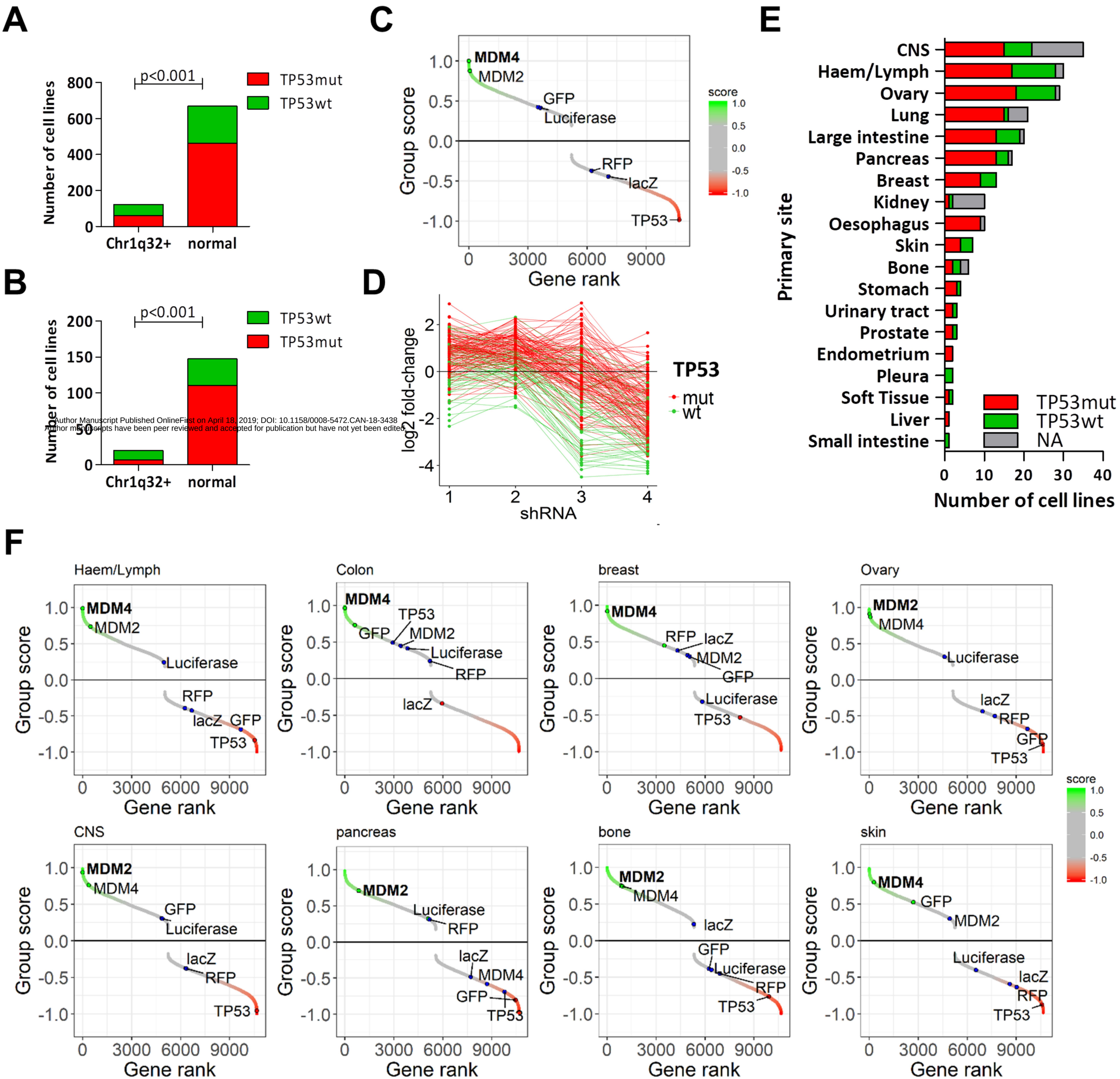

Author Manuscript Published OnlineFirst on April 18, 2019; DOI: 10.1158/0008-5472.CAN-18-3438
Author manuscripts have been peer reviewed and accepted for publication but have not yet been edited.

Cancer Research
The Journal of Cancer Research (1916–1930) | The American Journal of Cancer (1931–1940)

American Association for Cancer Research

MDM4 is targeted by 1q gain and drives disease in Burkitt lymphoma

Jennifer Hüllein, Mikolaj Slabicki, Maciej Rosolowski, et al.

Cancer Res Published OnlineFirst April 18, 2019.